Thermal effects on the hydraulic conductivity of a granular geomaterial

Effets thermiques sur la conductivité hydraulique d'un géomatériau granulaire

Marina S Bortolotto, David M G Taborda & Catherine O'Sullivan
Department of Civil and Environmental Engineering, Imperial College London, UK, marina.bortolotto@imperial.ac.uk

ABSTRACT: Geotechnical challenges arising from thermal loading are associated with many engineering applications such as ground source energy systems (5°C-40°C) and nuclear waste disposal (in excess of 100°C). The effects of temperature on soils have been the subject of limited research, particularly in terms of the fundamental characterisation of the non-isothermal behaviour of granular geomaterials. This study describes challenges associated with determining the hydraulic conductivity (k_h) of such materials at different temperatures using a bespoke temperature-controlled triaxial apparatus. A methodology is proposed for interpreting thermo-hydro-mechanical (THM) tests on isotropically consolidated specimens and is applied to data obtained for a uniform sand. It is shown that the intrinsic head losses of the system need to be minimised in order to obtain reliable measurements; this requires a detailed calibration procedure. The developed approach is used to determine the hydraulic conductivity at ambient temperature and at 40°C, showing that the increase in k_h with temperature is mostly due to the reduction in the viscosity of water. A detailed analysis of the volumetric response of the sample during heating is also carried out.

RÉSUMÉ : En envisageant les défis géotechniques de chargements thermiques associés à des applications d'ingénierie, comme ceux liés aux pompes de géothermie (5°C-40°C) et aux traitements de déchets nucléaires (> 100°C). Les effets de la température aux sols ont été sujet à des recherches limitées, en particulier concernant la caractérisation fondamentale du comportement non isothermique des matériaux granulaires. Cette étude décrit les défis spécialement associés à la détermination de la conductivité hydraulique (k_h) de matériaux différents utilisant une cellule triaxiale fait sur mesure pour le règlement de température. Une méthodologie est alors proposée pour l'interprétation de la réponse thermo-hydro-mécanique (THM) sur des échantillons consolidés de manière isotrope. Alors, cette méthodologie est appliquée sur des données recueillies en utilisant du sable uniforme. Il est démontré que les pertes de charges intrinsèques du système doivent être minimisées afin d'obtenir des fiables. Ceci nécessite une procédure de calibrage particulière. Cette approche développée est utilisée pour définir la conductivité hydraulique à température ambiante et à 40°C. Elle démontre une augmentation en k_h est due à une réduction de la viscosité de l'eau. Donc, une analyse détaillée de la réponse volumétrique lors du réchauffement de l'échantillon est effectuée.

KEYWORDS: thermo-hydro-mechanical behaviour, thermal loading, hydraulic conductivity, head loss, granular material

1 INTRODUCTION

Thermal loads imposed on geomaterials can originate from natural phenomena (e.g. weather changes) or human-made structures, such as buried pipelines and power cables, and nuclear waste repositories (Liu et al. 2018). Each heat source can result in different temperature fields. Although weather changes can be quite extreme (e.g. frost penetration), it is known that for depths greater than 10-15m, temperature within the soil mass becomes roughly constant throughout the year (Banks 2012). This constant temperature of the ground enables an effective heat exchange with a building through buried heat exchanger pipes (ground source energy system), which can heat or cool internal environments depending on the season. While these systems usually operate between 5°C and 40°C; nuclear waste repositories can impose temperatures in excess of 100°C, leading to vastly different technical challenges.

Although most of the mentioned applications (including those related to geothermal energy and nuclear waste disposal) can occur in granular geomaterials (i.e. sands and gravels), little attention has been given to characterising on the thermo-hydro-mechanical (THM) response of these materials.

A temperature-controlled triaxial apparatus (MKII cell) has been developed at Imperial College London and further adapted to perform hydraulic conductivity tests. The initial goal was to obtain high-quality data on the coupled THM behaviour of granular materials. The modification of this cell in order to perform hydraulic conductivity tests has proven to be very challenging, not only due to the complexity of temperature effects on the behaviour of the soil sample and the reliability of instrumentation, but also because of intrinsic hydraulic head losses arising from the fundamental design of the system. This paper provides a brief overview of the approach taken to overcome both challenges and reports initial results.

2 THERMAL TESTING ON SATURATED GRANULAR GEOMATERIALS

Mitchell & Campanella (1964) pioneered the investigation of the thermal behaviour of saturated soils using a triaxial apparatus modified for this purpose. The focus of the work by these authors was on clayey geomaterials. Since then, most studies and developed equipment have focused on finer grained materials (Liu et al. 2018), with very limited research dedicated to characterising the response of granular geomaterials to temperature changes.

Densification of dry granular materials – quartz sand (Kosar 1983) and glass beads (Chen et al. 2006) – was reported after specimens with different initial densities were subjected to cyclic thermal loads reaching temperatures up to 50°C. In both cases, the samples were loaded under one-dimensional conditions, which enabled an accurate measurement of the changes in volume. However, it is unclear whether any corrections were performed to account for the thermal expansion of the equipment.

Alternatively, temperature-controlled triaxial cells can be used to mitigate lateral boundary effects, in principle leading to a more accurate measurement of the response of the soil specimen. Ng et al. (2016) used a temperature-controlled triaxial cell to test Toyoura sand specimens at different densities and subjected to thermal loads. When loose and medium dense specimens of this sand (consolidated to a mean effective stress of

200 kPa) were heated to temperatures of 35°C, they exhibited contractive behaviour. Conversely, denser specimens exhibited only dilation under temperatures up to 50°C; this is most likely due to the thermal expansion of individual sand particles.

Hydraulic conductivity tests at various temperatures have been conducted in different apparatuses. However, similar to other aspects of the thermo-hydro-mechanical behaviour of geomaterials, the main focus has been fine-grained geomaterials. For instance, Delage et al. (2000) tested Boom clay in a temperature-controlled triaxial apparatus, while Towhata et al. (1993) tested kaolinite-like and bentonite clays in a temperature-controlled oedometer.

3 DEVELOPMENT OF APPARATUS

The detailed design of a temperature-controlled triaxial apparatuses can differ depending on the main desired outcomes and the characteristics of the geomaterials that are to be tested. The MKII cell is a bespoke apparatus that represents the latest design for temperature-controlled triaxial testing equipment developed at Imperial College London. Martinez-Calonge (2017) presents the previous version of the temperature-controlled triaxial (MKI). Fundamentally, the MKII cell can be understood as a regular (isothermal) triaxial apparatus positioned within a water bath (Figure 1). Two MKII cells were developed: a cell capable of shearing and a cell capable of performing hydraulic conductivity tests (herein designated as “permeameter”). This paper focusses on the permeameter.

3.1 Design

The entire apparatus is heated up by three 150W electric cartridge heaters, indicated in Figure 1 as (H3), which are placed in the water bath (3), i.e. between the triaxial cell (4) and the outer PVC jacket (2). The cartridge heaters are embedded into hollow brass rods which, due to the high thermal conductivity of this material, help to distribute heat more evenly.

The water bath is enclosed within the PVC jacket (2), and it is non-pressurised (i.e. at atmospheric pressure) and is included to enhance heat transfer between the heaters and the triaxial cell. A circulation pump (17) was added to the water bath to promote heat transfer through advection and impose a more uniform temperature field along the surface of the pressurised chamber (4). Without the circulation pump, larger temperature changes would tend to occur around the cartridge heaters, leading to substantial heterogeneity.

Using the heating system (H3) described the applied temperatures range from room/ambient temperature (20°C ± 2°C) to 85°C. Alternatively, the entire system can also be cooled down to temperatures below room temperature, to about 5°C by coupling an external cooling unit (“chiller”) to the system, using a similar strategy to that adopted for a temperature-controlled oedometer also developed at Imperial College London (Kirkham et al. 2018).

Temperature is measured at four points: inside the water bath (T1), inside the pressurised chamber (T2), inside the pedestal (T3), and externally (T4). The first three points (T1, T2 & T3) are essential as the system includes a substantial amount of water, which has a high heat capacity. Consequently, the entire system does not reach thermal equilibrium immediately and measurements closer to the sample are necessary. Moreover, because the PVC jacket is in contact with air, heat losses to the ambient cannot be avoided, further suggesting that additional internal measurements of temperature are required to understand the true temperature field being applied. In order to reduce heat loss to the ambient, a layer of polyethylene (closed cell) foam (1) surrounding the lateral surface and top of the PVC jacket was added. The temperature sensor T4 assesses the effect of radiation from the cell on key elements of the system (e.g. volume gauges and pore water pressure transducers)

Similar to the cartridge heaters, the temperature sensors (T1-T3) are embedded into hollow brass rods. For the inner cell temperature sensor (T2), the brass rod not only provides a physical barrier to water protection, but also isolates the sensor from pressurised water. All temperature sensors embedded into brass rods (T1- T3) are positioned at the extremity of the rod, matching roughly half of the height of the specimen and, therefore, providing more representative measurements of the specimen’s temperature.

Because the entire system is heated up, problems with instrumentation are inevitable. Internal instrumentation, in the form of LVDTs (Linear Variable Differential Transformer) (8), are normally glued to samples in order to obtain local measurements of displacements and, consequently, reliable strains at the small-strain range (shear strains about 10^{-6} m/m). The internal coil mechanisms of LVDTs are highly sensitive to temperature changes, with the operational temperature range of these components being quite narrow, particularly in the case of those with high resolution. This is currently an important obstacle which strongly limits the advance of temperature-controlled high-quality experimental testing, especially regarding the assessment of volumetric strains of a specimen subjected to thermal loads.

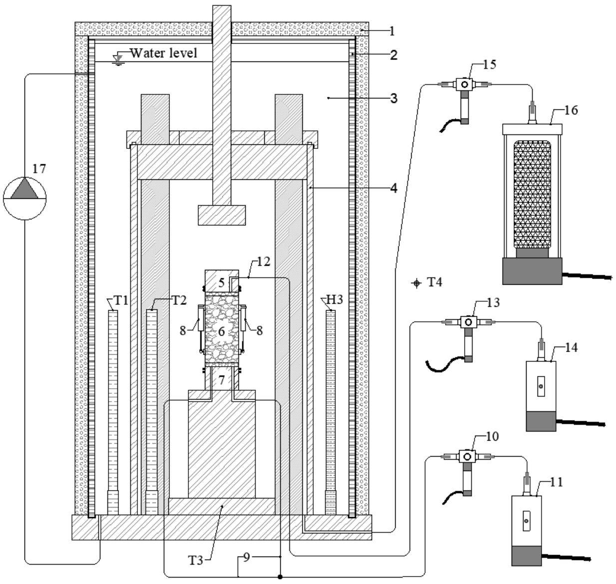

Figure 1. Schematic diagram of the temperature-controlled triaxial MKII cell at Imperial College London capable of measuring hydraulic conductivity. (1) polyethylene foam coat; (2) PVC jacket with a lid containing the water bath (non-pressurised); (3) water bath; (4) stainless steel triaxial pressurised chamber (up to 5MPa); (5) top cap; (6) soil specimen between two porous stones and filter papers; (7) pedestal; (8) two axial LVDTs; (9) two drainage lines connected to the bottom of specimen; (10) de-aired block & bottom back pressure pore water transducer; (11) bottom drainage line volume gauge; (12) drainage line connected to the top of specimen; (13) de-aired block & top back pressure pore water transducer; (14) top drainage line volume gauge; (15) cell pore water pressure transducer; (16) cell air-water interface; (17) circulation pump; (T1) water bath temperature sensor; (T2) inner cell temperature sensor; (T3) cell base temperature sensor; (T4) external temperature sensor; (H3) heater number 3 (out of 3 equally spaced around the pressurised chamber).

The apparatus is considered a high pressure triaxial apparatus as it can apply total stresses of up to 5MPa. There are three independent pressure control systems each with its own air-water interface: (11), (14) & (16) referring to the bottom and top back pressures (of the specimen), and the cell pressure, respectively.

The back pressure air-water interfaces are 100 cm^3 Imperial College-type volume gauges that are not only capable of applying pressure but also measuring changes in volume. Each system has its individual pore water pressure transducer (10, 13 & 15). Hydraulic gradients can be applied to the specimen (allowing hydraulic conductivity tests) because the control systems of (9) and (12) are independent.

Unlike a conventional permeameter, where pore water pressure measurements are taken exactly at the bottom and top of the specimen, the pore water pressure transducers in the MKII cell are positioned away from the warm parts of the equipment. However, this approach leads to longer drainage lines and more frictional head loss. In comparison to the case for finer-grained materials, head losses in hydraulic conductivity tests on granular materials using triaxial cells are important due to the higher velocities being recorded in the system, i.e. relatively lower head loss in the samples themselves. Further details about head losses are presented in Section 3.2.

While specimens 50mm in diameter and 100mm in height (6) were tested in the current study, the cell was designed to also accommodate 100x200mm (diameter x height) specimens by replacing both top cap (5) and pedestal (7). These components (top cap and pedestal) are made out of 316L stainless steel, which is characterised by higher corrosion resistance.

Two drainage lines are connected to the pedestal (9) and both are used while saturating, consolidating and performing hydraulic conductivity tests. The top cap is connected to only one drainage line (12). Nylon tubes with an internal diameter of 1.43 mm are used in all drainage lines, with the exception of the portions of drainage lines that are inside the pedestal and top cap, which have an internal diameter of 3.05mm.

Bauxite porous stones were initially used since small thermal expansion values were desired. However, this material was found to generate very high head losses during hydraulic conductivity tests. Consequently, these were replaced by new sintered bronze porous stones which are more porous and therefore impose smaller head losses, despite the expected larger thermal expansion of these elements.

Another aspect that has been shown to be of fundamental importance was the material comprising the membrane placed around the specimen. Preliminary tests confirmed the conclusions of Martinez-Calonge (2017) who used the MKI cell, and found that neoprene membranes should be employed to avoid problems arising from the degradation of latex under elevated temperatures.

3.2 Intrinsic head losses

Head (1998) states that hydraulic conductivity tests conducted in a triaxial cell are inevitably affected by head losses (i.e. pressure losses) that take places along the tubes (frictional parcel) or at fittings, valves and changes in diameter. Both of these components – distributed or localised – are proportional to the square of the velocity of the fluid, v.

Since faster flow rates are expected while testing granular materials, head losses in the apparatus (herein designated as "intrinsic") can be comparable or even larger than those within the specimen. As a result, the determination of hydraulic conductivity becomes more complex with additional calibration required to account for these head losses. An empirical approach based on that presented by Head (1998) has been developed for the interpretation of the results obtained using the MKII cell.

The intrinsic head loss of the system was obtained by placing the two porous stones between the top cap and the pedestal, separated by a single sheet of filter paper. After flushing, the system was saturated and pressure differences ranging from 2 kPa to 20 kPa were applied across the system.

The measured pressure differences between the top and bottom pore water pressure transducers are plotted against the measured flow rate in Figure 2. The obtained relationship describes the system's intrinsic head loss (measured in terms of pressure differential, Δp_l) for each flow rate, which should be subtracted from the value measured (Δp_{meas}) when conducting tests with a soil specimen. The obtained corrected value ($\Delta p_{cor} = \Delta p_{meas} - \Delta p_l$) should then be used to calculate the hydraulic gradient when determining the hydraulic conductivity using Darcy's law.

In Figure 2, solid lines represent the system's intrinsic head losses (calibration curves) for different temperatures. Dashed lines represent the combined response of the system and soil specimen, which require correction as described above. It is important to highlight that the combined system and soil curves must necessarily be below the calibration curves, indicating a 'positive' head loss at the specimen. Any other behaviour indicates that head losses in the system are so large that no discernible head loss in the specimen can be determined, preventing determination of the hydraulic conductivity.

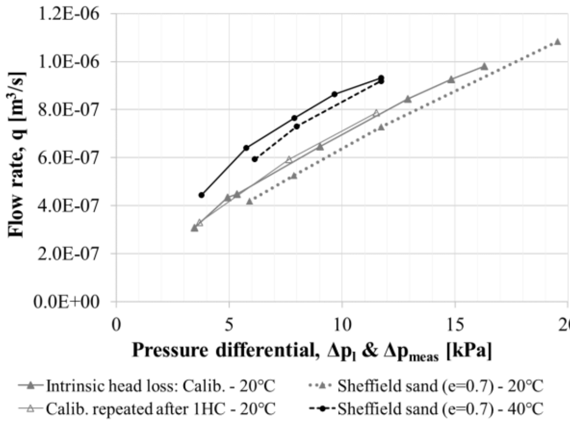

Figure 2. System's intrinsic head loss calibration curves with temperature (solid lines) and hydraulic conductivity tests curves on Sheffield sand (dashed lines) consolidated at 100 kPa (e=0.70) without any head loss correction. All curves refer to upwards flow with constant head loss tests conducted in a triaxial apparatus (MKII cell).

It should be noted that the ASTM D5084 - 16a (ASTM 2016) requires that, for a given applied pressure, the head loss of the system should be less than a tenth of the system and soil combined. Since this standard is applicable to soils with an hydraulic conductivity up to $1 \cdot 10^{-5}$ m/s (i.e. relatively low flow rates), it is believed that this limit was established to enable hydraulic conductivity measurements without requiring any head loss corrections.

Since the expected hydraulic conductivities of the granular materials to be tested using the MK II cell are greater than $1 \cdot 10^{-5}$ m/s, head losses had to be minimised. A theoretical analysis showed that the largest proportion of the head losses in MKII cell was related to the frictional component, indicating that a possible mitigation for this would be to reduce the length or increase the internal diameter of the piping used in the setup.

A systematic approach was undertaken in order to minimise, where possible, the intrinsic frictional head loss of the system. The first step was to double (approximately) the internal diameter of all drainage lines (from 0.73 mm to 1.43mm), reducing the flow velocity. Subsequently, new sintered bronze porous stones were used, which were observed to generate half the head loss of the previously employed bauxite porous stones. Lastly, the two original drainage lines (one at the bottom and one at the top of the sample) were shortened by about 30% ; this had only a minor impact on the system response. However the addition of a second drainage line to the bottom of the specimen had a significant impact on the measured head losses.

Although the current system configuration did not achieve the desired ratio of 10 between the response of the system and that combined response of system and soil, the insight achieved in its development enabled a robust procedure for correcting the results. This procedure relies on the calibration curves shown in Figure 2. As expected, when testing at elevated temperatures the system's intrinsic head losses reduces (i.e. for a given pressure differential, a higher flow rate is obtained) due to a reduction in the viscosity of water. In the following section, an example of the procedure followed to interpret the obtained data is given.

4 HYDRAULIC CONDUCTIVITY OF SHEFFIELD SAND

4.1 Sheffield sand

Sheffield sand is a fine non-plastic sand with 4% of fines. The fines content and particle size distribution were obtained through manual-wet sieving. Additional physical characteristics are presented in Table 1, with both coefficients of uniformity (C_u) and curvature (C_z) indicating that this is a roughly uniform sand.

Table 1. Sheffield sand characterisation

G_s	e_{min}	e_{min}	D_{50} [mm]	C_u	C_z
2.68	0.63	0.97	0.196	1.91	0.98

4.2 Methodology

The specimen was set up by dry deposition using a funnel and then flushed with freshly de-aired water (using a volume of water at least twice the volume of voids) from bottom to top by applying a small hydraulic gradient across the sample. Saturation was achieved by ramping up both back pressure (controlled by the bottom volume gauge) and cell pressure at a rate of 1.1 kPa/min until the target back pressure (500 kPa) was achieved, with 30 kPa of effective stress. After achieving a B-value higher than 0.92, the specimen was allowed to consolidate under an effective stress of 100 kPa.

After consolidation, hydraulic conductivity tests were performed following the guidelines in ASTM D5084 - 16a (ASTM 2016) for flexible wall permeameters using constant head. Four to six increasing hydraulic gradients (stages) were applied while ensuring that the effective stress level at mid-height of the sample remained unchanged. To achieve this, the headwater pressure (higher pressure) was always applied to the specimen first and only then the tailwater pressure (effluent) was applied. This procedure was observed to lead to the best system response, despite the temporary reduction in effective stress applied to the specimen.

Pressure differentials ranging from 4 kPa to 16 kPa were applied to the specimen since smaller values (~2 kPa) were difficult to control with sufficient accuracy, and higher pressure differentials (>16 kPa) could lead to excessively high flow rates. It is important to note that, in accordance with ASTM D5084 - 16a (ASTM 2016), the maximum pressure differential should be limited to about 2 kPa; this value is recommended for soils with hydraulic conductivities between $1\cdot10^{-5}$ m/s and $1\cdot10^{-6}$ m/s. In the case of Sheffield sand, the hydraulic conductivity is expected to be considerably higher, meaning that smaller pressure differentials should be applied in order to keep the flow rates sufficiently low. However, in addition to the difficulties associated with applying such low pressure values with sufficient accuracy, it should be noted that even the highest pressure difference applied (16 kPa) represents only 8% of the effective stress since half of the pressure difference is increased from the initial value of back pressure (500 kPa). This is within the limit of a 95% increase in headwater pressure normalised by the effective stress level, as specified in the same standard.

Consecutive stages of upwards and downwards flow were performed, since one of the volume gauges was always empty at the end of each stage in a specific direction. For simplicity, only results regarding upwards flow are presented and discussed here.

The measured combined response of the system and specimen is given by dashed curves in Figure 2. These were corrected using the procedure described above and the hydraulic conductivity values (k_h) were then calculated using Darcy's law (Eq. 1).

$$k_h = \frac{q}{A \cdot i} = \frac{q}{A \cdot {}^{\Delta p_{cor}}/_{\gamma_w \cdot L}} \tag{1}$$

where k_h is the hydraulic conductivity [m/s], q is the flow rate [m^3/s], A is the cross-sectional area [m^2], i is the hydraulic gradient, Δp_{cor} is the corrected pressure differential [kPa], L is the specimen height during the hydraulic conductivity tests [m] and γ_w is the unit weight of water $[kN/m^3]$. The volumes measured by both volume gauges were in good agreement and so the average of both values was used in Eq. 1.

After conducting hydraulic conductivity tests at room temperature, the system was heated up to 40°C. Thermal equilibrium was judged to be attained once the sample volume changes stabilised. Subsequently, the same procedure for performing hydraulic conductivity at room temperature was followed, using the system calibration curve for 40°C.

A simple methodology for was developed based on that proposed by Campanella & Mitchell (1968). According to this approach, the volume of water measured by the volume gauge ($V_{drained}$) represents the excess volume of water that, after thermal expansion, exceeds the volume of voids. Clearly, individual sand particles, the soil skeleton as a whole, and the water dilate with temperature. It is assumed that the changes in the volume of voids due to temperature changes will be described by the same coefficient of thermal expansion as that of the individual soil particles. As a result, in this idealised scenario where no particle rearrangement takes place, thermal strains do not result in changes in void ratio. Building upon this assumption, it is possible to estimate the theoretical volume of water that should leave the sample due to the larger thermal expansion of water as $V_{V,0} \cdot (\alpha_W - \alpha_S) \cdot \Delta T$, with $V_{V,0}$ being the initial volume of voids $[m^3]$, α_W and α_S the volumetric coefficients of thermal expansion of water and particles [m/(m K)], respectively, and ΔT the applied change in temperature $[K]$. Any deviation of the observed response from this idealised scenario indicates the existence of thermally-induced mechanical strains which are associated with particle rearrangement and, thus, with changes in void ratio. In effect, by comparing the expected volume of water that should leave the sample to that measured by the volume gauge ($V_{drained}$), it is possible to infer the change in the volume of voids caused by particle rearrangement (herein designated as "mechanical strain", ε_m), as shown in Eq. 2. As the degree of saturation is 100%, then the initial volume of voids is equal to that of water in the specimen.

$$V_{drained} = V_{V,0} \cdot (\alpha_W - \alpha_S) \cdot \Delta T + \varepsilon_m \cdot V_0 \tag{2}$$

An updated value for the volume of voids is obtained:

$$V_V = V_{V,0} \cdot (1 + \alpha_S \cdot \Delta T) - \varepsilon_m \cdot V_0 \tag{3}$$

Eq. 2 is rearranged to get an expression for ε_m, using this expression and Eq. 3 the change in void ratio Δe can be determined through Eq. 4, given an initial value for this quantity e_0:

$$\Delta e = e_0 \cdot \left[\frac{(\alpha_W - \alpha_S)\cdot\Delta T - \frac{V_{drained}}{V_{W,0}}}{(1+\alpha_S\cdot\Delta T)}\right] \quad (4)$$

It should be noted that an increase in temperature also affects the pore fluid's density and viscosity. One option to investigate the different factors contributing to variations in hydraulic conductivity due to temperature changes is to consider the intrinsic permeability (K_i):

$$k_{h,T} = \frac{K_i \cdot \gamma_{w,T}}{\mu_{w,T}} \quad (5)$$

where $k_{h,T}, \gamma_{w,T}$ and $\mu_{w,T}$ are the hydraulic conductivity $[m/s]$, the unit weight of water $[N/m^3]$ and the dynamic viscosity of water $[Pa \cdot s]$ at a given temperature T $[K]$, respectively, and K_i is the intrinsic permeability $[m^2]$.

4.3 Results

Hydraulic conductivity tests were performed on a specimen of Sheffield sand with a relative density of 80.5% (e=0.70) and consolidated under 100 kPa of effective stress.

4.3.1 Tests at room temperature

The hydraulic conductivity at room temperature, obtained following the methodology described above is presented in Table 2. Moreover, theoretical predictions of hydraulic conductivity from the literature based on the physical characteristics of the sample are also included. Clearly, although these estimates are consistently lower than the measured value, the differences are small.

Table 2. Hydraulic conductivity at room temperature for Sheffield sand: measured values using constant head method (upwards flow), and theoretical methods base on semi-empirical approaches

Source / Methodology		γ_d *[kN/m³]*	k_h *[m/s]*
Measured	Present study	15.5	$2.60 \cdot 10^{-4}$
	Chapuis (2004)		$8.66 \cdot 10^{-5}$
Theoretical	Hazen (1892, 1911)	15.5	$9.91 \cdot 10^{-5}$
	Terzaghi (1925)		$1.79 \cdot 10^{-4}$

4.3.2 Tests at elevated temperature

Hydraulic conductivity tests were conducted at 40°C and the observed response was corrected using the calibration curve for 40°C shown in Figure 2. The applied hydraulic gradient was increased systematically from 4 kPa to 12 kPa and the stability of the specimen pressure did not reach the high levels seen at ambient temperature. Furthermore, at 40°C, the difference between the responses of the system and that of the system and specimen combined are significantly smaller, particularly for larger hydraulic gradients. To be conservative only the two lower pressure differentials (~4 and 6 kPa) were used to determine the hydraulic conductivity, which is presented in Fig. 3. Further research is required to investigate the effect of large flow rates at elevated temperatures.

It is interesting to note that for both investigated temperatures, the actual hydraulic gradients applied to the specimen (after correcting for the intrinsic head loss) range from about 1.0 to 1.29, which is in agreement with the maximum suggested value by ASTM D5084 - 16a (ASTM 2016). The roughly constant difference between the calibration curves and the data that include the specimen suggests that friction effects are still affecting the system, i.e. the head losses in the system are still excessively large, meaning that further investigation is required.

As expected, a larger hydraulic conductivity was observed for higher temperatures (Fig. 3), agreeing with results obtained by e.g. Towhata et al. (1993) for normally consolidated kaolinite-like and bentonite clays. The variation of this property with temperature, as previously explained, includes several factors, such as the temperature-dependence of the density and viscosity of water and the changes in the soil skeleton. In order to isolate the effects of the various factors, the intrinsic permeability, which has been shown to be relatively independent of temperature (e.g. Delage et al. (2000)), was determined. For the Sheffield sand considered here a very slight reduction of the value of this property from 20°C to 40°C was obtained. Considering that the hydraulic conductivity increased, this reduction in intrinsic permeability suggests that the dominant factor is that of the changes in water viscosity with temperature. Furthermore, since the variation is very small (from $2.64 \cdot 10^{-11}$ to $1.91 \cdot 10^{-11}$ m²), further testing is required at a range of temperatures to establish definite conclusions on this issue.

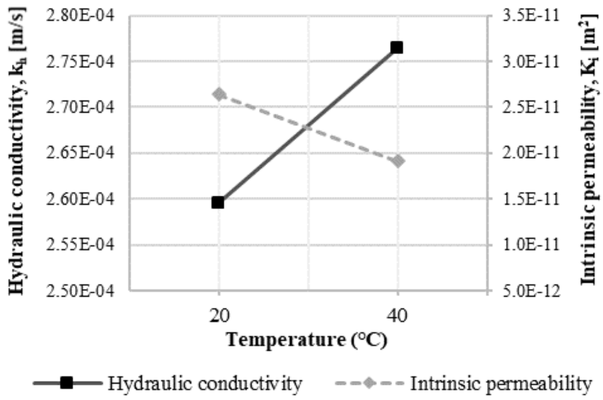

Figure 3. Hydraulic conductivity and intrinsic permeability of Sheffield sand (e=0.70) subjected to effective stress of 100 kPa at 20°C to 40°C

It was noticed that warm water (i.e. at a temperature higher than ambient) reaches pore water pressure transducers and, most likely, volume gauges as well. Despite the assumed ingress of this warmer water, there is still a good agreement between the two volume gauges and it appears not to affect the accuracy of the testing procedure. The effects on the pore water pressure transducers, however, are more evident. Chen, Zdravkovic & Carraro (2019) presented evidence that, for their system, the performance of pore water transducers is not greatly affected by temperatures within a range of 21°C to 60°C while performing calibration under high temperatures (virtually no flow). Clearly, hydraulic conductivity tests on sandy materials are characterised by higher flow rates and thus this effect may become more important, requiring further research.

4.3.3 Volume changes with temperature

Describing non-isothermal volume changes is essential to understand the thermal response of granular materials. When heating up a specimen, water drained out of or into the volume gauge represents the combined thermal response of the specimen and the system.

When heating the specimen from 20°C to 40°C, an excess volume of water of about $1.9 \cdot 10^{-7}$ m³ going into the volume gauge was measured. Without accounting for the system's thermal expansion, an issue which requires further investigation and calibration, the interpretative method described above (Eq. 2 to 4) was used to characterise the deformation of the specimen under thermal loading.

Based on the obtained results and assumed properties for the thermal expansion of fluid and soil particles ($\alpha_{W,40°C}$=1.00 $\cdot 10^{-5}$ m/(m K) and α_S=$1.26 \cdot 10^{-4}$ m/(m K)), a compressive mechanical strain of $1.06 \cdot 10^{-4}$ % was calculated. These are strains that are assumed to correspond to changes in the soil skeleton, suggesting that particle rearrangement has taken place when individual particles expanded due to the increase in temperature. It is essential to account for the contribution of the fluid expansion, since calculating the volumetric strains using the classical approach of drained water divided by the initial specimen volume would have resulted in a volumetric strain of about $-1.06 \cdot 10^{-1}$ % (dilation), which is three order of magnitudes higher than what is believed to be the actual mechanical strains occurring within the soil specimen. Such small mechanical strains result in very limited changes to the void ratio, further explaining the very small variation in intrinsic permeability observed during the heating process. Naturally, the overall specimen volume increased considerably during the heating stage, due to the thermal expansion of the individual soil particles. The measured value is in accordance with the results reported by Delage et al. (2000) and Ng et al. (2016). In particularly, it compares well with the volumetric strains obtained by Ng et al. (2016) for Toyoura sand in a dense state (D_r = 90%), where dilation is mainly proportional to the thermal expansion of individual sand particles.

5 CONCLUSIONS

This paper introduces an on-going research study focusing on generating, measuring and interpreting high-quality experimental data on the complex THM behaviour of granular media. A temperature-controlled triaxial apparatus (MKII cell) has been developed at Imperial College London to perform hydraulic conductivity tests at different temperatures. This has been challenging since the design requirements for non-isothermal testing tend to generate greater intrinsic head losses. In order to minimise these head losses, the following modifications were implemented (the values in brackets represent the gain in flow rate when compared to previous configuration): doubling the internal diameter of drainage lines (3.7), introducing sintered bronze stones (2.0), reducing the total length of tubes by about 30% (1.1), and adding a second drainage line to the bottom of the specimen (2.0). The combination of all these solutions resulted in a flow rate approximately 14 times higher than the original one for the same pressure differential. However, these solutions increased the water volume within drainage lines, which may introduce difficulties when determining volume changes under non-isothermal conditions. This will be the subject of further investigation.

A methodology for interpreting the complex THM behaviour of saturated media has been described which relies only on the measurements of the water volume flowing into or out of the volume gauge. This approach allows the estimation of the mechanical strains which are assumed to reflect the changes in particle arrangement and hence the only driver for changes in void ratio. However, internal instrumentation, which until now has shown to be highly affected by temperature changes, is essential to validate this methodology, as well as to measure the total volumetric strain of the specimen. As discussed before, the lack of internal instrumentation with high resolution and wider operational temperature range is limiting the advance of temperature-controlled high-quality experimental testing.

A good agreement between theoretical and measured hydraulic conductivity values of a Sheffield sand specimen (σ'=100 kPa and e=0.70) was found at room temperature (20℃ ± 2℃). This suggests that the proposed empirical correction for the system's intrinsic head losses is adequate. It should also be noted that without the proposed approach, the hydraulic conductivity would have been determined to be two orders of magnitude lower, which is a considerable error. Although less stable at higher temperatures, the current configuration of the MKII cell demonstrated to be capable of generating reliable results of hydraulic conductivity at 40 ℃ (±0.5℃). With respect to effects of temperature on intrinsic permeability, further evidence corresponding to at least one additional temperature is required. However, based on current results, it appears that the main factor influencing the hydraulic conductivity is the variation with temperature of the viscosity of water.

6 ACKNOWLEDGEMENTS

This project is funded through Marie SKŁODOWSKA-CURIE Innovative Training Network MATHEGRAM, the People Programme (Marie SKŁODOWSKA-CURIE Actions) of the European Union's Horizon 2020 Programme H2020 under REA grant agreement No. 813202.

7 REFERENCES

ASTM. 2016. *D5084-16a: Standard test methods for measurement of hydraulic conductivity of saturated porous materials using a flexible wall permeameter*, ASTM International, United States of America.

Banks, D. 2012. *An introduction to thermogeology - Ground source heating and cooling*, 2nd ed. John Wiley & Son Ltd., United Kingdom.

Campanella, R.G. and Mitchell, J.K. 1968. Influence of temperature variations on soil behaviour. *ASCE Journal Soil Mechanics and Foundation Engineering Division* 4(3), 709-734.

Chapuis, R.P. 2004. Predicting the saturated hydraulic conductivity of sand and gravel using effective diameter and void ratio. *Canadian Geotechnical Journal* 41(5), 787-795.

Chen, K., Cole, J., Conger, C., Draskovic, J. Lohr, M., Klien, K., Scheidemantel, T., and Schiffer, P. 2006. Packing grains by thermal cycling. *Nature* 442, 257–257.

Chen, S., Zdravkovic, L. & Carraro, J.A.H. 2019. Thermally induced pore water pressure of reconstituted London clay. *E3S Web Conf. 92(2019), Proc. 7th International Symposium on Deformation Characteristics of Geomaterials*, Glasgow, 1-5.

Delage, P., Sultan, N. and Cui, Y.J. 2000. On the thermal consolidation of Boom clay. *Canadian Geotechnical Journal* 37(2), 343–354.

Hazen, A. 1892. Some physical properties of sands and gravels, with special reference to their use in filtration. *24th Annual Report, Massachusetts State Board of Health*, United States of America.

Hazen, A. 1911. Discussion of 'Dams on sand foundations' by A. C. Koening. *Transactions of the American Society of Civil Engineers* 73, 199-203.

Head, K.H. 1998. *Manual of soil laboratory testing. Volume 3: Effective stress tests*, 2nd ed. John Wiley & Sons Ltd., England.

Kirkham, A.D., Tsiampousi, A. & Potts, D.M. 2018. Temperature-controlled oedometer testing on compacted bentonite. *Proc. 7th International Conference on Unsaturated Soils*, Hong Kong, 6.

Kosar, K.M. 1983. *The effect of heated foundations on oil sand*, MSc Thesis, University of Alberta, 248p.

Liu, H., Liu, H., Xiao, Y. and McCartney, J.S. 2018. Influence of temperature on the volume change behavior of saturated sand. *Geotechnical Testing Journal* 41(4), 747–758.

Martinez-Calonge, D. 2017. *Thermo-mechanical behaviour and thermal properties of London clay*, PhD Thesis, Imperial College London, 277p.

Mitchell, J.K. and Campanella, R.G. 1964. Creep studies on saturated clays. *In Laboratory Shear Testing of Soils*, edited by ASTM Committee D-18, West Conshohocken, 90-103.

Ng, C.W.W., Wang, S.H. and Zhou, C. 2016. Volume change behaviour of saturated sand under thermal cycles. *Géotechnique Letters* 6(2), 124–131.

Towhata, I., Kuntiwattanaku, P., Seko, I. and Ohishi, K. 1993. Volume change of clays induced by heating as observed in consolidation tests. *Soils and Foundations* 33(4), 170–183.